17th Brazilian Congress of Thermal Sciences and Engineering
November 25th-28th, 2018, Águas de Lindóia, SP, Brazil

ENCIT-2018-0286
BACKGROUND-ORIENTED SCHLIEREN IN A YALE BURNER

Bernardo Luiz Harry Diniz Lemos
Vítor Augusto Andreghetto Bortolin
Rodrigo de Lima Amaral
Guenther Carlos Krieger Filho
Universidade de São Paulo, Escola Politécnica, Engenharia Mecânica – Av. Professor Mello Moraes 2231, Cidade Universitária. São Paulo/SP. Brazil.
bernardolemos@usp.br; vitorbortolin0@gmail.com; rodrigoamaral@usp.br; guenther@usp.br

Abstract. *Combustion may be the first technique mastered by the humankind and until today, it is essential for the society. However, there is a lot more to understand about combustion, either by its basic concepts or by the frontiers of the knowledge. The study of reactive flows is useful to improve machines using CFD simulation and experiments. In experimental investigations, imaging techniques use sensors (CCD or CMOS) and a light source to extract information from the flow, such as temperature and velocity. However, the variation of the refractive index caused by the chemical reaction deteriorates the measurements of most of the imaging techniques applied in combustion. In order to improve the combustion technology, this paper tested the applicability of the background-oriented schlieren (BOS), a quantitative technique that use the variation of the refractive index as a signal to extract information of the flow. In this investigation, the Yale coflow was chosen because it is a reference burner for academic purposes and has many different data measured by distinct experiments. The experiment conditions tested in the present paper were laminar and lifted flame with five distinct backgrounds. These experiments were done in order to investigate the background importance, the pixel displacement in each background, the signal to noise ratio and window resolution in the particle image velocimetry algorithm. The random white dots in a black background and the transparency with random black dots proved to better options in both cases.*

Keywords: *background-oriented schlieren, Yale burner, combustion*

1. INTRODUCTION

Combustion plays an important role for humankind, either during the cooking of a food in a propane or natural gas stove or firewood, or during daily driving in a car or bus driven by an internal combustion engine, or yet a plane trip with their turbines. However, these machines do not work properly in all kind of scenarios. In order to improve efficiency and functionality in different ranges, experimental tests are done to new parts and also to answer some questions about the operation principle.

Testing an apparatus is not an easy task, various variables can disturb an experiment, and therefore many tests are done in a simplified version of the original apparatus in a controlled environment. For example, it is possible to test a whole gas turbine, but if the concern is only in the burner, this part is tested alone to minimize errors. Nevertheless, to perform correctly a test, the experimental technique used must be validated, either by comparing it with other technique(s), numerical simulation or by analytical solutions. If a new technique arises, it will be compared with a well establish method, usually in simple and known experiment. In this line of thought, the Yale coflow burner is a known experiment in combustion media and can be used to verify if a new technique has data similar to the others.

Conventional optical diagnostic techniques applied in reactive flows are Particle Image Velocimetry (PIV), Laser Doppler Velocimetry (LDV) or Anemometry (LDA), Raman scattering, Coherent Anti-Stokes Raman Spectroscopy (CARS), Rayleigh scattering, Generalized Lorenz-Mie Theory (GLMT), Laser-Induced Fluorescence (LIF), Laser-Induced Phosphorescence (LIP), Laser-Induced Incandescence (LII), and Schlieren techniques. PIV and LDV/LDA are used to measure the velocity of the fluids through tracer particles. On the other hand, Raman scattering and CARS are used to measure the concentration of chemical species. CARS, Rayleigh scattering, LIF and LIP are used to obtain temperature measurements. Measurements of the droplet size are obtained by GLMT. Soot formation is characterized by LII. Finally, Schlieren techniques are applied mainly for fluid structure and density visualization. One thing that these entire optical techniques have in common is that all must use a laser beam, and laser beans for experiments are expensive.

Beside the cost of the laser apparatus, each technique mentioned above has its particular limitation when applied to reactive flows. First, the PIV needs seed particles that flows inside the reactive flow, but these particles must not burn, or the information will be lost. In order to avoid then burning and still keep it luminosity inside the flame, researchers have been using thermographic phosphors particles, like BAM:Eu^{+2}, Mg_4FGeO_6:Mn and La_2O_2S:Eu. The concern about these particles are namely, the size of the particles are below 2μm, which may cause pneumoconiosis. In addition, there is the

concern about the discard of toxic heavy metals present in the thermographic phosphors in air and/or water without a proper precaution. Furthermore, even these phosphorous particles are not able to provide enough signal for flame temperatures above 900 K (FOND, YIN, *et al.*, 2016). Finally, the variation of density in the flow creates distortions in the PIV images.

In addition to the problem with seeding particles, LDA has a strong disadvantage of being a one-point sampling technique, which means that this technique is zero-dimensional when most flows have tree-dimensional velocities. Alongside this factor, LDV suffers from nonuniform seeding in flames that lead to errors (CHIGIER, 1991). Subsequently, Raman scattering and spectroscopy are influenced by seed particles when it is done together with other technique, like PIV or LDA, or soot; beam steering and defocusing. (CHIGIER, 1991) Rayleigh scattering has a limitation in refractive index that must be close to one. LIF and LIP require florescent and phosphorous materials that may be introduced in the flow or applied as a thermo-coating in the burner or surroundings. These materials must have a well-known luminescence half-life in order to predict the temperature fluctuations in the experiments. Schlieren techniques have the great advantage of the absence of laser, but in some cases, it will require concave mirrors that can be expensive and sometimes is no quantitative. Background Oriented Schlieren (BOS) is a recent developed technique when compared to the first Schlieren technique and also have its limitations. BOS relies on the variation of the refractive index of the medium to extract information from the flow pattern based on its background.

2. OBJECTIVES

The main objective of this paper is study the influence of four variables in the BOS technique during reactive flow experiments. These variables are the background pattern, pixel displacement between the background and flow recording, signal to noise ratio (SNR) and window resolution in particle image velocimetry (PIV) algorithm that is used to process the BOS images. Further, the present paper will discuss the positive and negative aspects of BOS.

3. BACKGROUND-ORIENTED SCHLIEREN (BOS)

Schlieren are optical non-homogeneities in a transparent material, not always visible to the human eye. Schlieren imaging systems visualize fluctuations in optical density in a qualitative way. The basic experimental apparatus required are: a light source, a pair of plano-convex lenses, a disturbance in a flow, a sharp knife-edge and a camera, all positioned according to the lens focus. Another type of schlieren uses parabolic mirrors instead of lenses. (SETTLES and HARGATHER, 2017)

The Schlieren technique is widely used in experiments that involve fluids because it is not intrusive, therefore, it does not affect the system to be measured. One of the constraints of the system is size, because of the dependence of the focal length and the mirror size, since they are dependent variables in the system assembly. The other problem is portability of the constructed system. The mirrors and other apparatus used in the assembly of the schlieren technique are fixed, since different distances require different mirrors and/or focal lengths according to (MAZUMDAR, 2013).

In the 1930s the German engineer Hubert Schardin discovered the background distortion during schlieren photography, but at the time he was not able to process the images due to the lack of technology. However, the 21st century brought the computer era thus algorithms could be done a lot faster than before. In addition, scientists wanted a quantitative way to measure flows. With these ideas in mind, (DALZIEL, HUGHES e SUTHERLAND, 2000) and (RAFFEL, RICHARD e MEIER, 2000) created the background-oriented schlieren (BOS). BOS is a synthetic schlieren technique that do not require mirrors. Therefore, the entire system relies on variation of the refractive index, background pattern and digital image processing. The differences in experimental apparatus between the conventional schlieren and BOS are the absence of lens/mirrors and the presence of a random dot-pattern background, which makes BOS cheaper and less complex. The background can be generated by a computer software and it can be composed by dots in a regular distribution or randomly. Besides the dots, there is the wavelet-noise background (GUO and LIU, 2017). These three computer generated backgrounds must have a high contrast in order to the minimize errors in image correlation. In the other hand, it is possible to use natural backgrounds, such as sand in deserts, trees or rocks (RAFFEL, 2015).

Before the experiment begins, the image of the background is taken. After that, the test can start and multiple frames are recorded in the memory of a high-speed camera. Each image taken by the camera in the BOS setup has a shifted dot of the background in the image plane, when compared with the first image without fluid flow, as stated by Settles and Hargather (2017). This shift is caused by a variation in refractive index. To correctly measure the displacement of the dot, the size of the background, the dot distribution and the focal distance of the camera are important. For example, returning to Figure 1, ε_y is the refraction angle in the y coordinate. As the dot-pattern size in x and y background are known, as well as the focal distance in z, a simple trigonometry can be done:

$$\Delta x = \frac{Z_D \cdot Z_I}{Z_B} \cdot \frac{1}{n_0} \cdot \int_{Z_D-\Delta Z_D}^{Z_D+\Delta Z_D} \frac{\partial n}{\partial x} dz \tag{1}$$

$$\Delta y = \frac{Z_D \cdot Z_I}{Z_B} \cdot \frac{1}{n_0} \cdot \int_{Z_D-\Delta Z_D}^{Z_D+\Delta Z_D} \frac{\partial n}{\partial y} dz \tag{2}$$

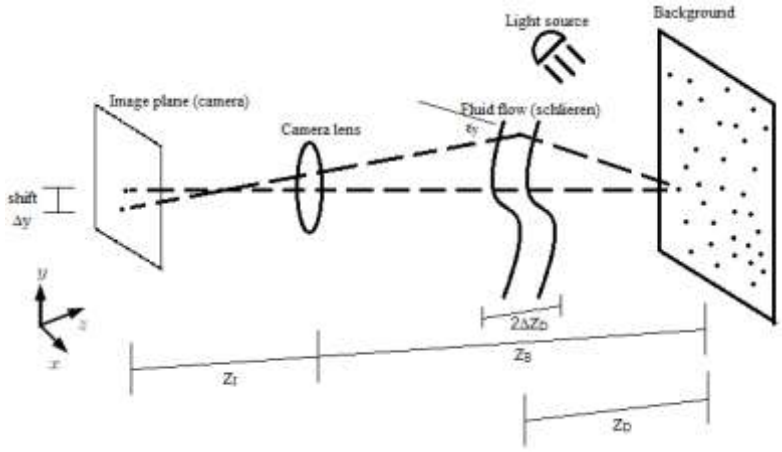

Figure 1 – Background-oriented schlieren

Where: Δx, the dot displacement in the horizontal coordinate; Δy the dot displacement in the vertical coordinate; Z_D, the distance from background to the fluid flow; Z_B, the distance between the background and the camera lens; Z_I, the distance between the lens and the image plane; n, the refractive index; n_0, the reference refractive index; ΔZ_D, the half distance of fluid flows; and z is the depth of view.

In addition, the Gladstone-Dale equation relates the density of a fluid and its refractive index:

$$n = 1 + K_{GD} \cdot \rho \tag{3}$$

Where K_{GD} is a constant dependent of the wavelength and ρ is the fluid density.

When the experiment is finished, all images are evaluated in an image correlation software, like MATLAB. Most of commercial and educational softwares are based on particle image velocimetry (PIV) algorithms, as stated by (RAFFEL, 2015)

BOS technique may be quantitative in some cases, which is a remarkable feature. For example, the refraction angle of a thermal boundary layer in a heated flat plated was compared using five different approaches: theoretical calculation, conventional calibrated schlieren with knife-edge cutoff, calibrated schlieren with graded-filter cutoff, rainbow schlieren and BOS. Excepting rainbow schlieren that has a considerable difference from theoretical calculation in the beginning of the heated plate, the other three quantitative methods exhibited a great concordance with the theoretical calculation. (HARGATHER and SETTLES, 2012)

Another example of BOS quantitative measurement was done in a vertical round hydrogen jet. In this experiment, hydrogen gas (H2) had a mass flow of 3 g/s, temperature of 290 K and velocity of 100 m/s. In this case, BOS technique was applied to this test to measure the concentration of H2 in different axial positions after the jet exit. As a result, BOS data has and error varying from 2.0 (close to the jet exit) to 12.3% (far from the jet exit) in comparison with a gas analyzer probe in the same axial positions. (KOTCHOURKO, KUZNETSOV, *et al.*, 2014)

In addition, BOS technique was employed to measure the temperature of a candle. To reconstruct the density, the Poisson equation was solved together with Gladstone-Dale equation. However, the temperature reconstruction is dependent of the pressure, according to gas state equation. Assuming an isobaric process, the temperature pressure relation is easily solved. Subsequently, the temperature field generated by the software based on the BOS images had a maximum error of 1.85% when compared with a digital thermometer in the same places. (GUO and LIU, 2017)

4. EXPERIMENTAL METHOD

The Yale burner (Figure 2a) is a diffusion flame, atmospheric pressure, axisymmetric burner with a coflow. It was developed in 1998 by McEnally et al. to study soot formation using thermocouples for temperature measurements and soot deposition. In addition, he has done laser-induced incandescence (LII) with Rayleigh scattering to create a temperature field. (MCENALLY, SCHAFFER, *et al.*, 1998)

In Figure 2b, the Yale burner fabricated at University of São Paulo is detailed as:

a) Coflow aluminum housing, which limits the air flow, has an external diameter of 89 mm and internal diameter of 73 mm;
b) Bottom plate has an external diameter of 130 mm;
c) Fuel tube made of stainless steel has an external diameter of 4.5 mm and thickness of 0.3 mm;
d) Honeycomb to relaminarize the air flow has an external diameter of 76 mm and 5 mm of thickness;
e) O-ring of 82.27 mm of internal diameter and 1.78 mm of cross section;
f) Air connections;
g) M6 washer;
h) M6 nut;
i) Allen M6x20 mm bolt;

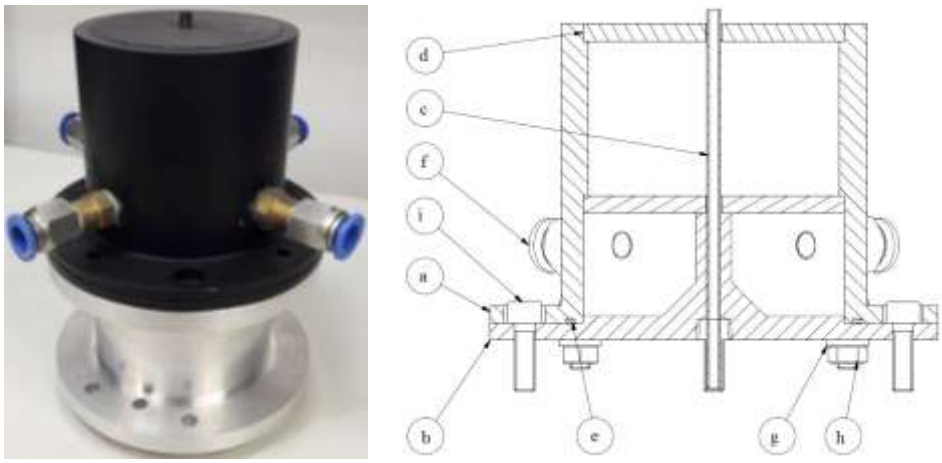

(a) (b)

Figure 2 – Yale burner

The experimental apparatus (Figure 3) that will be used to evaluate the BOS technique in the liquefied petroleum gas (LPG) air flame of the Yale coflow burner are:

a) The Yale coflow burner;
b) A high-speed camera;
c) A high power LED;
d) Multiple random dot backgrounds attached in an aluminum sheet.

The distance between the background and the center tube of the Yale burner, where the flame starts, is 140 mm, and the distance from the center tube to the camera lens is 200 mm. The bottom of the background has a height of 85 mm in relation to the center tube.

Two conditions were studied using the Yale burner, the laminar flame and the lifted flame, both premixed flames. Liquefied petroleum gas (LPG), which include mixes of propane (C_3H_8) and butane (C_4H_{10}) was chosen as fuel for the flames. The premixed gas chosen, as well as the coflow, was air. Flow conditions used to achieve these two events were measured using rotameters and the values are shown in Table 1.

Table 1 – Flow conditions for each event

Event	Flame type	Fuel flow	Premixed air flow	Coflow
1	Laminar	0,30 L/min (1)	1,75 L/min	60 L/min
2	Lifted	7,00 L/min (1)	1,75 L/min	70 L/min

(1) Rotameter values were set for air, so LPG values need correction

A high-speed camera used was a Phantom Miro 311 monochromatic (1200 x 800 pixels, 1000 Hz). The high power LED was placed above the camera, as can be seen in Figure 3, to project a strong illumination on background.

The background was generated in MATLAB by *makebospattern*, a toolbox of PIVmat. (MOISY, 2012). It is possible to configure some variables of the background, namely the number of dots in the background; the dot size in millimeters; and dot color, black or white. Beside the dot's variables mentioned above, other aspect tested in this work was the type of paper where the background was printed, tracing paper and transparency (cellulose acetate). Five distinct backgrounds were tested (see Table 2).

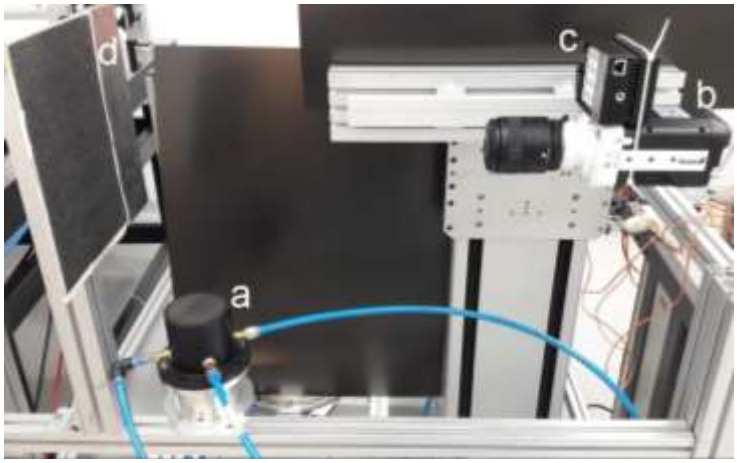

Figure 3 – Yale experiment assembly

Table 2 – Distinct BOS' background configurations

Case	Number of dots	Diameter of dots	Color of dots	Paper type
A	100 000	0,5 mm	Black	Tracing paper
B	100 000	0,5 mm	White	Tracing paper
C	50 000	0,5 mm	Black	Tracing paper
D	50 000	1,0 mm	Black	Tracing paper
E	100 000	0,5 mm	Black	Transparency

These backgrounds in different papers were tested in order to evaluate which one is the best for Yale's flow characteristics. The aluminum sheet has two major functions, a place where the background will attach and reflect part of the light emitted by the LED.

After the assembly, as image calibrator was placed above the Yale burner, and 100 images at 1000 Hz were recorded. Subsequently, the calibrator was removed and again 100 images at the same rate were recorded. This approach was used to make a good image mean and remove some fluctuations that may appear in the calibration and background images. Later, images of fluid flow and flames were recorded at a rate of 1000 Hz, varying from 1000 to 4000 images saved for each event. All images recorded were saved as Tagged Image File Format (TIF), an uncompressed file, in order to avoid losing information.

Background images were renamed as odd images and fluid flow images were renamed as even images to create pairs of original background and distorted background that were processed in PRANA/MATLAB. (ECKSTEIN *et al.*, 2008)

PRANA is an open-source graphical user interface (GUI) program for calculating velocity fields using Particle Image Velocimetry (PIV) or Particle Tracking Velocimetry (PTV). As mentioned before, PIV algorithm fits properly for BOS, thus pixel displacement will be calculated by PRANA. To process the images, first, the images directory must be loaded to PRANA in "Images and Data I/O" tab. Thereafter, the "Image Frame Step" was changed to "2" to ensure that only the background and the distorted background will be compared. All physical parameters were set as "1", so all the results will be displaced in pixels. Continuing the setup, now in "PIV Processing", the "Multigrid – DWO" was chosen with three or four passes. Inside "Pass Configuration" box in "Grid and Correlation Setup" the grid was specified in each pass with window resolution of 128x128 px, 64x64 px, 32x32 px and 16x16 px with window overlay of 50% for 128 px and 75% for other resolutions. In all passes, the Standard Cross Correlation (SCC) with three point Gaussian estimator was selected. Finally, before run current job, the "Postprocessing and Output" tab must be verified to guarantee that results will be saved in addition to the peak magnitude and, as PRANA calls, the velocity.

PRANA results were written in .mat format, an archive that include variables, functions, arrays and other information native to MATLAB. All the results were then read by a code developed by the authors in order to generate pixel displacement fields.

5. RESULTS

The distribution of the image displacement between the background and the flow can be used to assess the sensitivity of the approach. In this case, the BOS technique is more sensitive the greater the calculated image displacement in the PIV correlation.

Figure 4 shows the image displacement in the radial (Vr) and axial (Vax) directions for case 1A (subtitled in Table 1 and 2). In this case, an interrogation window size of 16 px was used.

The spatial resolution of BOS follows the same behavior as the PIV approach. The spatial resolution depends on the size of the sensor, particle image density and the interrogation window in the processing. The smaller the interrogation window, the larger the spatial resolution. PIV simulations show that some noise is generated when the number of pairs of particle images correlated by interrogation window is less than five. In BOS, another limiting point is the low variation of the refractive index in some directions. This problem is similar to the low dynamic velocity range (DVR) found in PIV. This makes it difficult to choose an ideal interframe time to properly correlate displacements in all directions. (ADRIAN and WESTERWEEL, 2011)

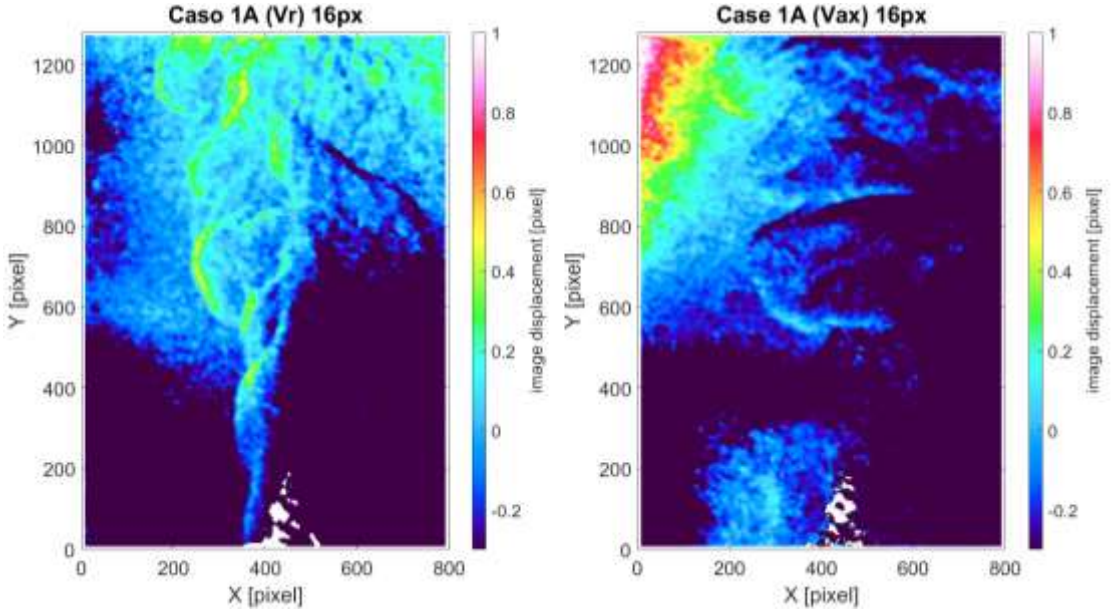

Figure 4 – Radial and axial image displacement for Case 1A (16px)

For Case 1A, Figure 5, Figure 6 and Figure 7 show the same velocities in grid windows resolutions of 32px, 64px and 128px respectively. It is possible to notice that the image with more interrogation resolution displacement and, subsequently, with more flow information is the one with 16px grid window resolution (Figure 4) and the worst image is the 128px grid (Figure 7). The white blur that can be seen in the bottom of some figures is the tip of the flame, and because of its brightness, PRANA was not able to match the pixel displacement.

It can be noticed that in Case 1A the radial image displacement is bigger than the axial image displacement because, in the Yale burner the density changes due to flame temperature differential in axial direction.

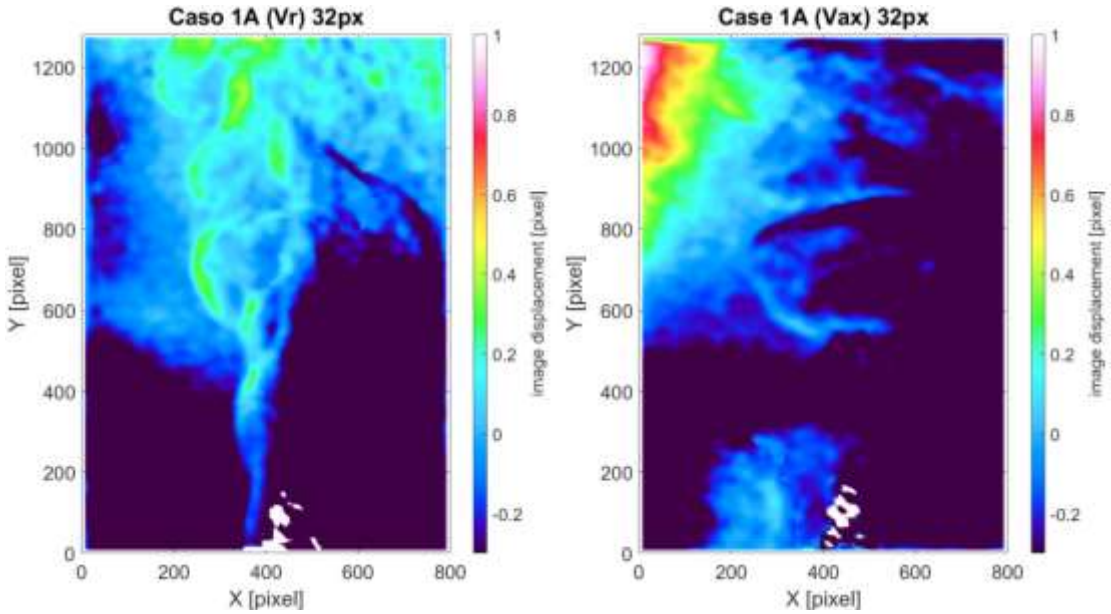

Figure 5 – Radial and axial image displacement of Case 1A in 32px

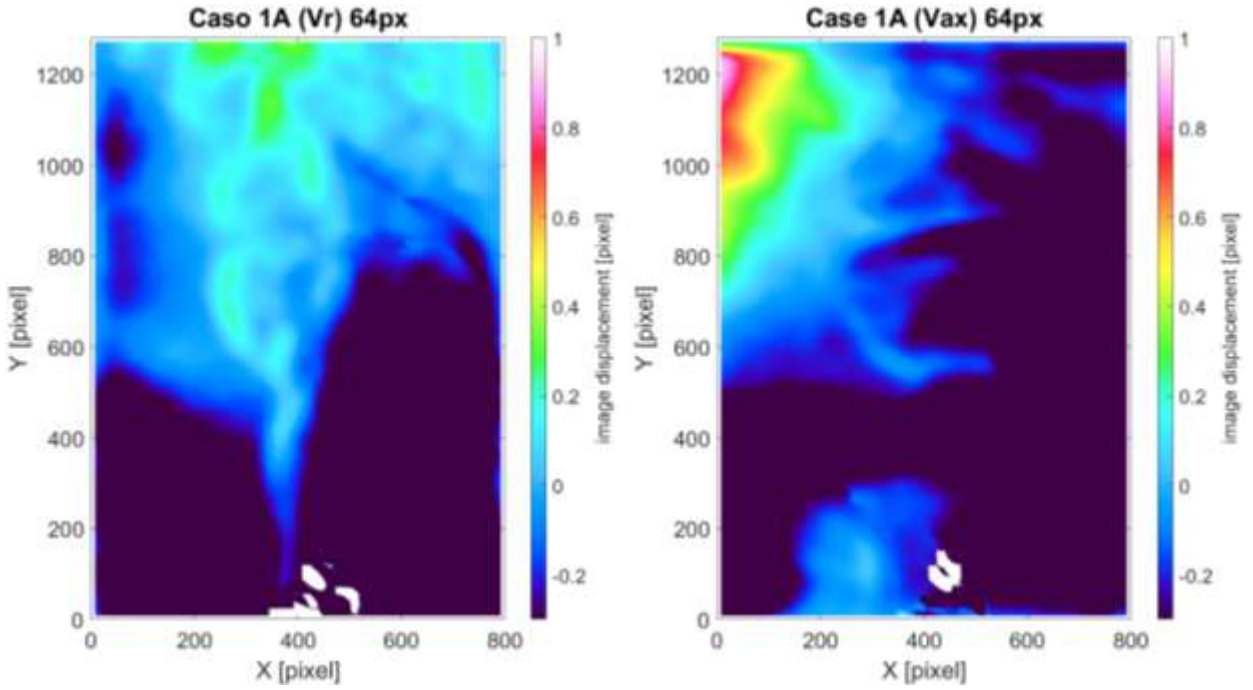

Figure 6 – Radial and axial image displacement for Case 1A (64px)

Another point that stands out in the Case 1A fields is the red blur present on top left image of axial image displacement. This red blur may be the absence of adhesive tape in this part of the background. Care must be taken with vibrations caused by the flame and / or fluid flow as they may move the background and cause distortion during experiments.

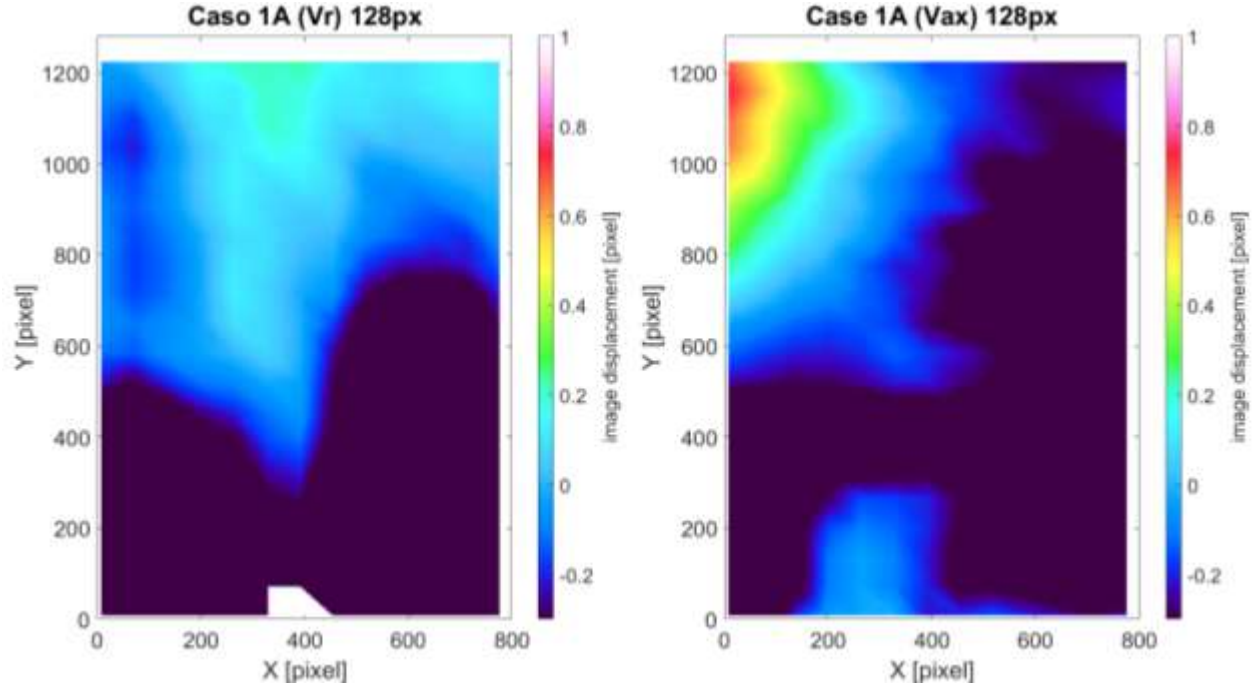

Figure 7 – Radial and axial image displacement for Case 1A (128px)

Evaluating the signal to noise ratio (SNR) of the Case 1A for 16px and 128px (Figure 8) it can be remarked that SNR value in the region where de density variation occurs is above 3 in both grid window resolution, however in 128px this is

more prominent. Although the SNR value is acceptable, value that informs if the data recorded is noise or not, in the 128px the image (Figure 7) does not shows how the flow behaves.

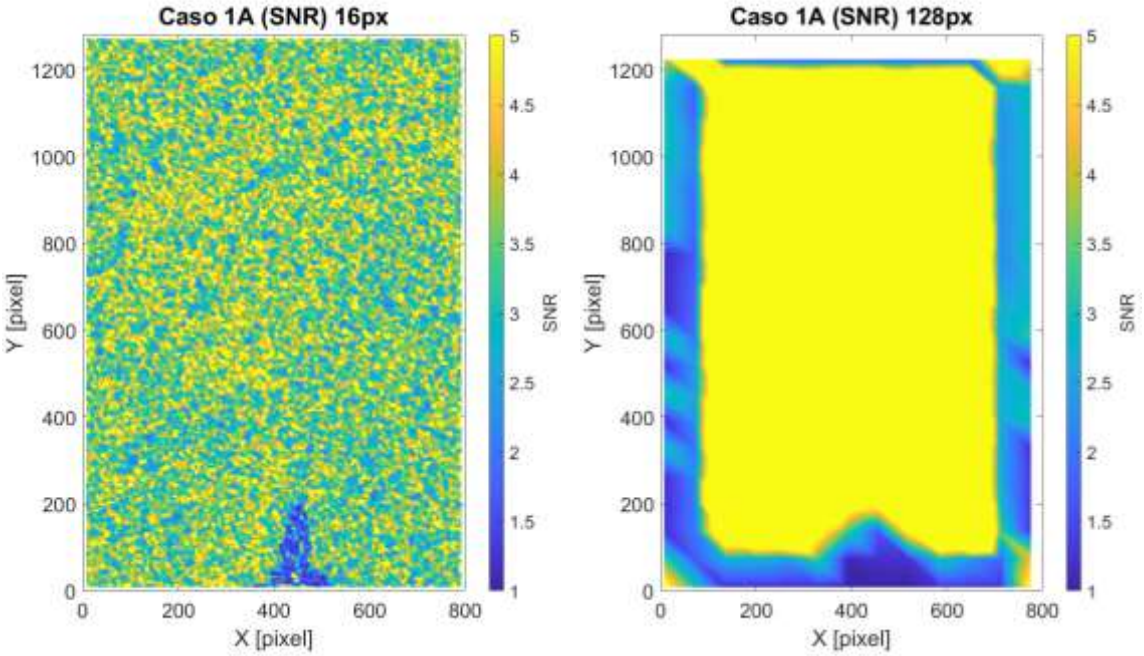

Figure 8 – Image displacement magnitude and SNR for Case 1A (16px and 128px)

In contrast to Case 1A, the Case 1B in Figure 9 shows a significant axial image displacement with a shape similar to the radial image displacement, despite its smaller displacement.

As mentioned before, the 16px image is the best to see the information of the flow, so, Figure 9 shows the image displacement for Case 1B. The same approach was applied to Figure 10, Figure 11 and Figure 12, which shown the image displacement of Cases 1C, 1D and 1E.

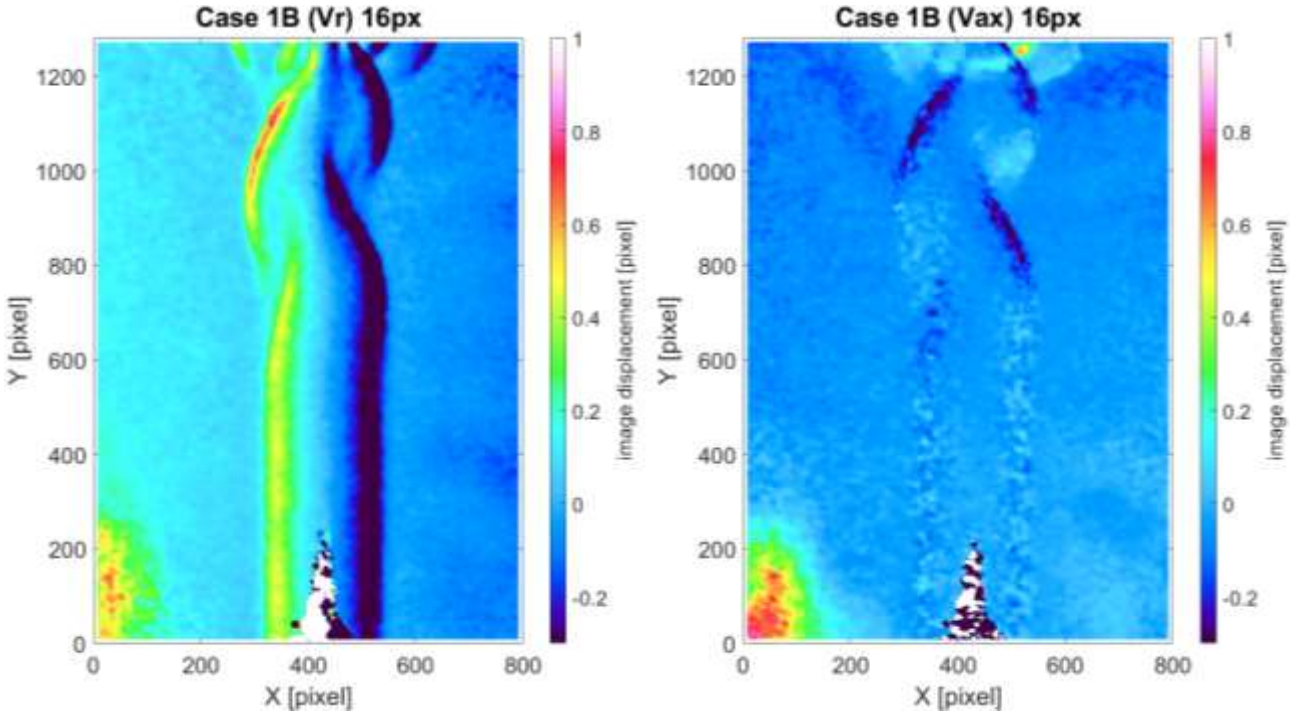

Figure 9 – Radial and axial image displacement for Case 1B (16px)

Figure 10 shows the pixel displacement of Case 1C. In this particular case, the density change is not well visible, even for the radial image displacement that can be only noticed in the top part of the left figure.

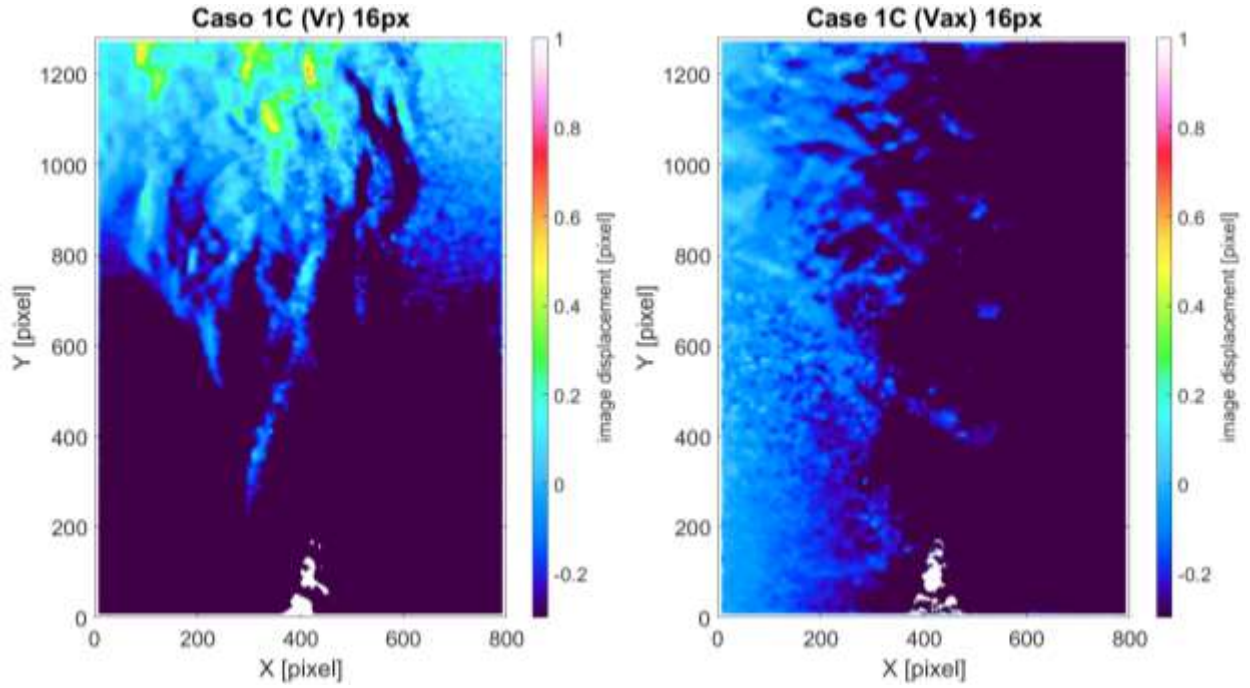

Figure 10 – Radial and axial image displacement for Case 1C (16px)

In Figure 11, the Case 1D shows a remarkable density gradient in both radial and axial velocity with visible turbulent structures.

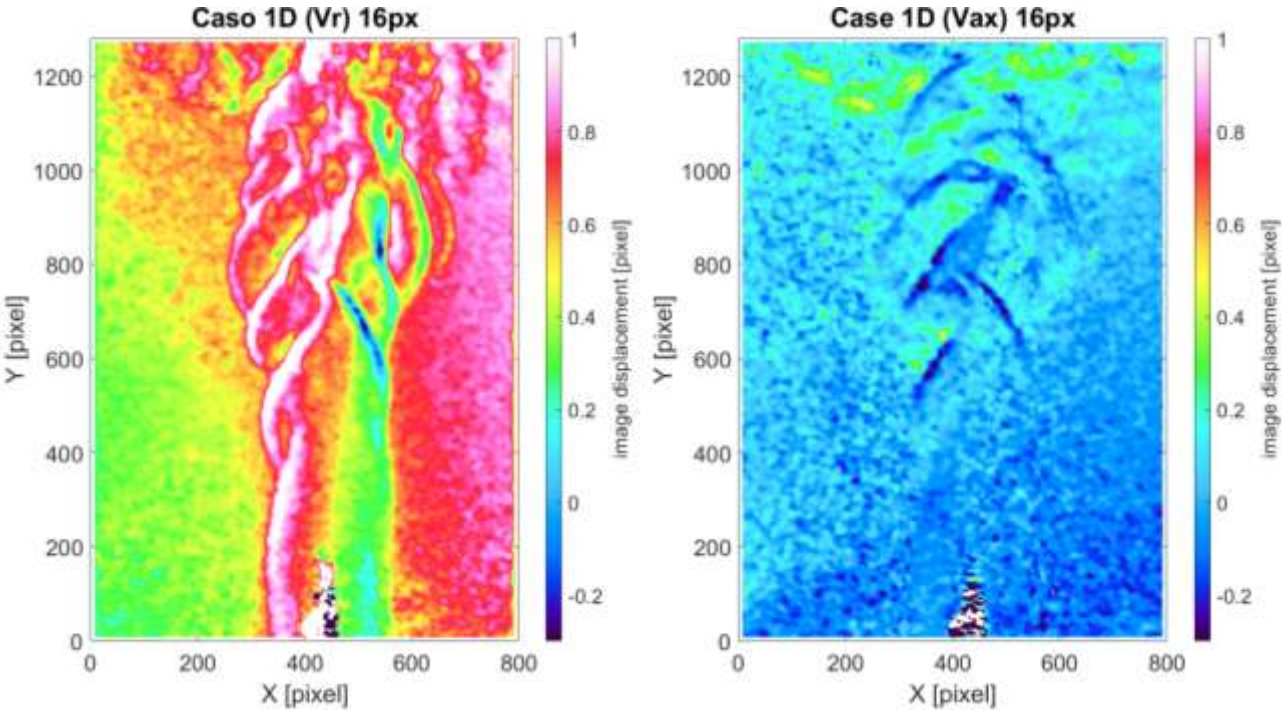

Figure 11 – Radial and axial image displacement for Case 1D (16px)

The transparency used in Case 1E, in addition to the aluminum sheet, generated (Figure 12) a good shape of the hot air macro structures above the laminar flame.

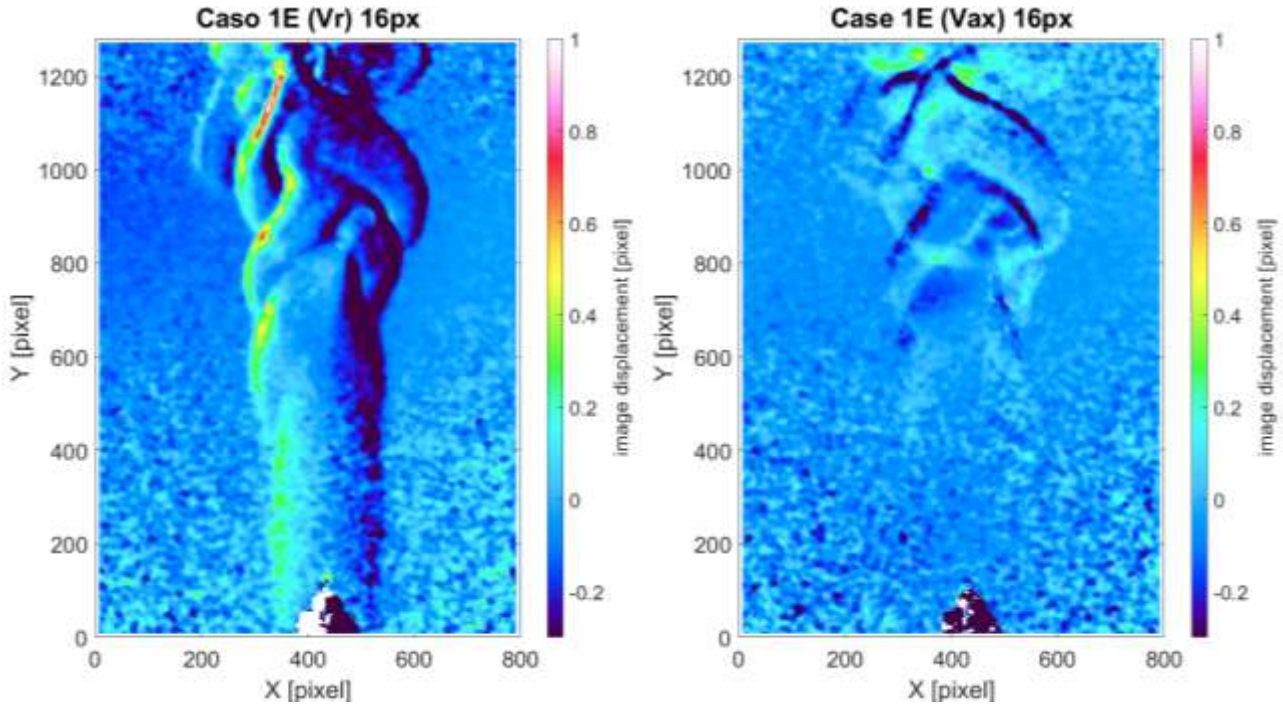

Figure 12 – Radial and axial image displacement for Case 1E (16px)

When compared, the five events with the laminar flame it can be perceived that the Cases B, D and E have a better overall fluid flow information, when compared to Cases A and C. In Case B, the transition between the density that has changed and the density that remained the same is smoother, as can been seen by the low gradient in the horizontal lines. On the other hand, in Case D, it is possible to spot the highest pixel displacement (red color). Finally, in Case E in the region between 640 and 960 pixels in Y axis, the transition is smoother than in other parts of the figure due to the reflection of the LEDs in the aluminum sheet in this region that caused a better correlation among the background and the distorted image.

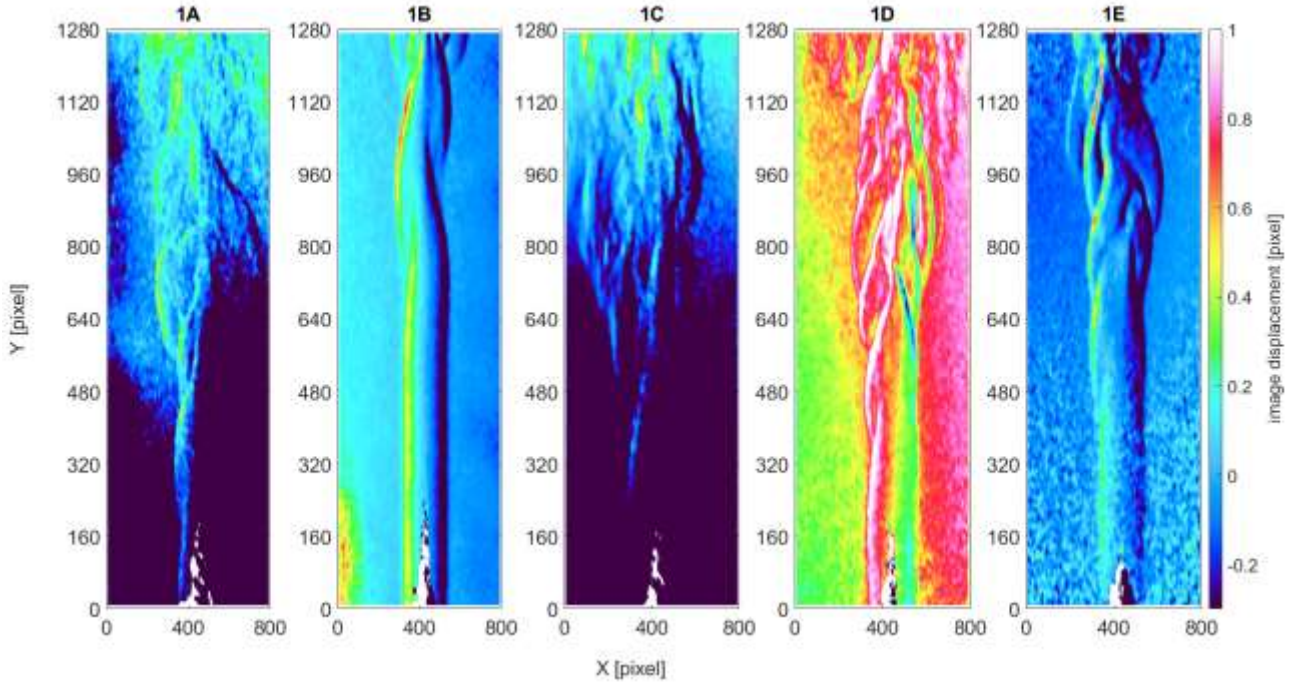

Figure 13 – Multiple cases of laminar flame compared (16px)

In Figure 14, the velocity magnitude for each case was plotted.

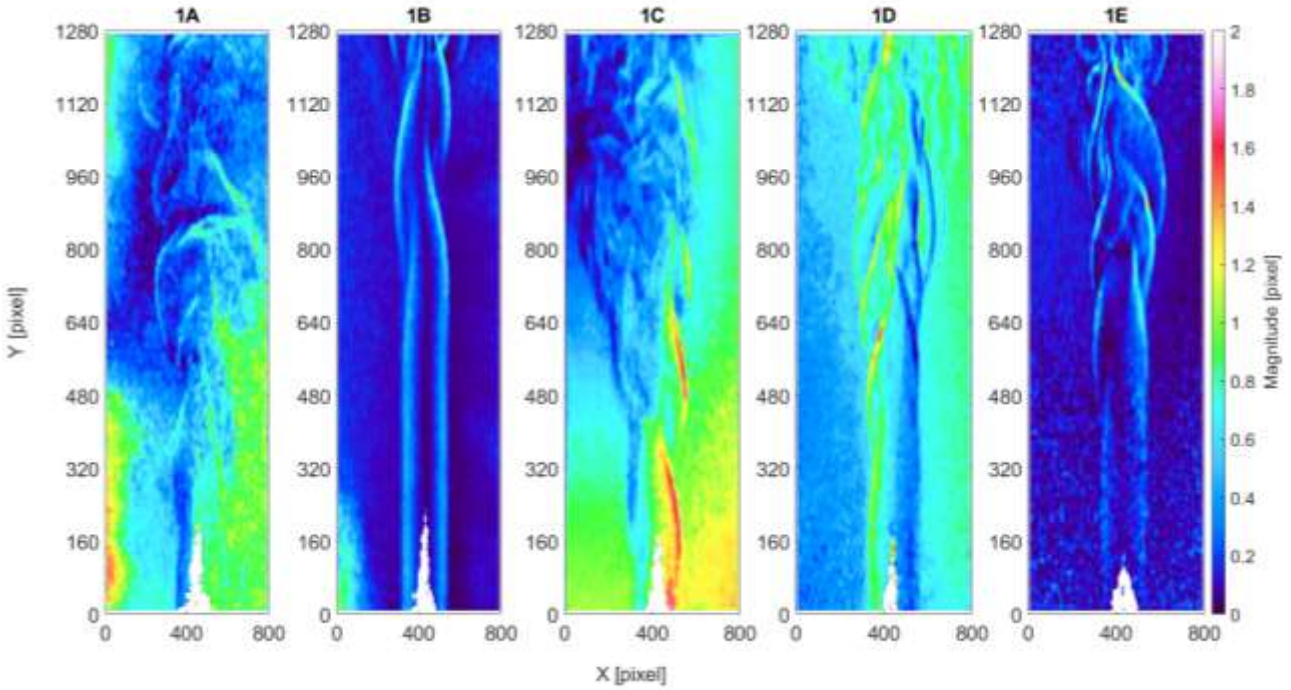

Figure 14 – Image displacement magnitude for multiple laminar flame cases (16px)

The interesting part of this plot are the Cases A and C. Both cases show another perspective of the fluid flow captured by BOS, especially for Case C whose magnitude changed its obscure view near the flame to a complete view.

Afterward, the transient condition lifted flame in BOS was analyzed for four cases, namely, the cases A, B, C and E.

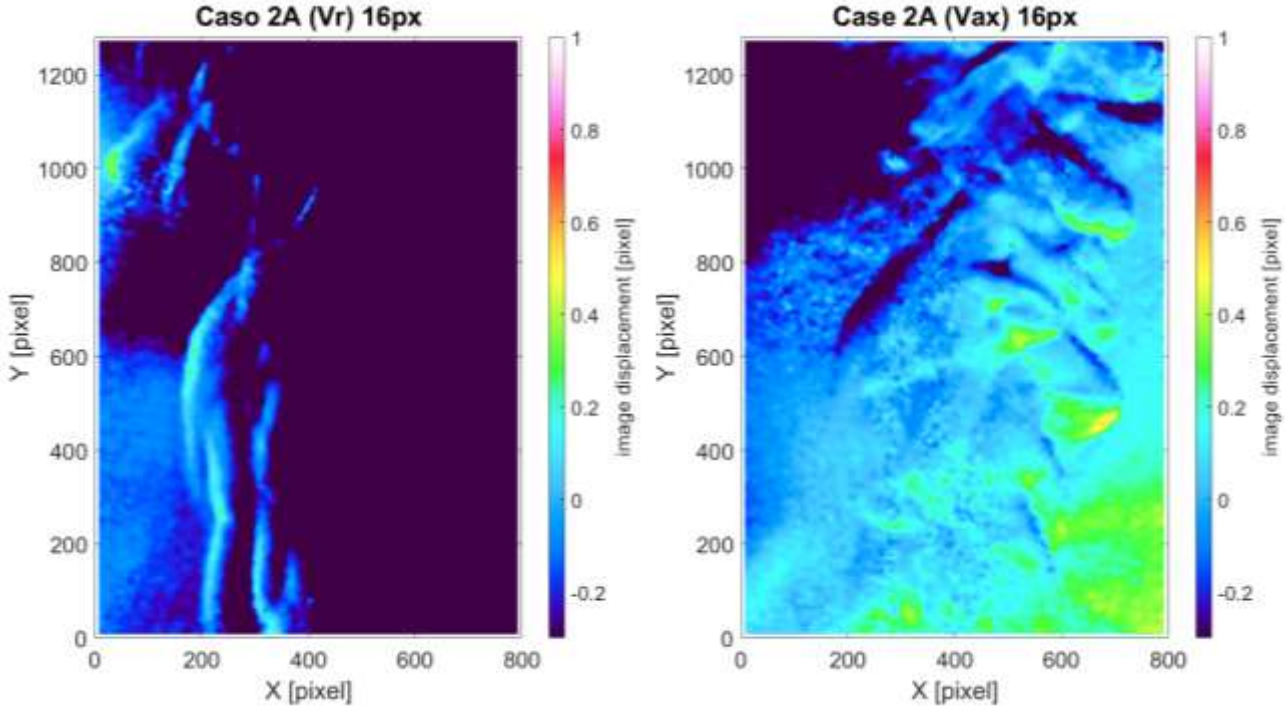

Figure 15 – Radial and axial image displacement for Case 2A (16px)

Starting with Case 2A (Figure 15) and 2B (Figure 16), where the images shows small displacements (blue).

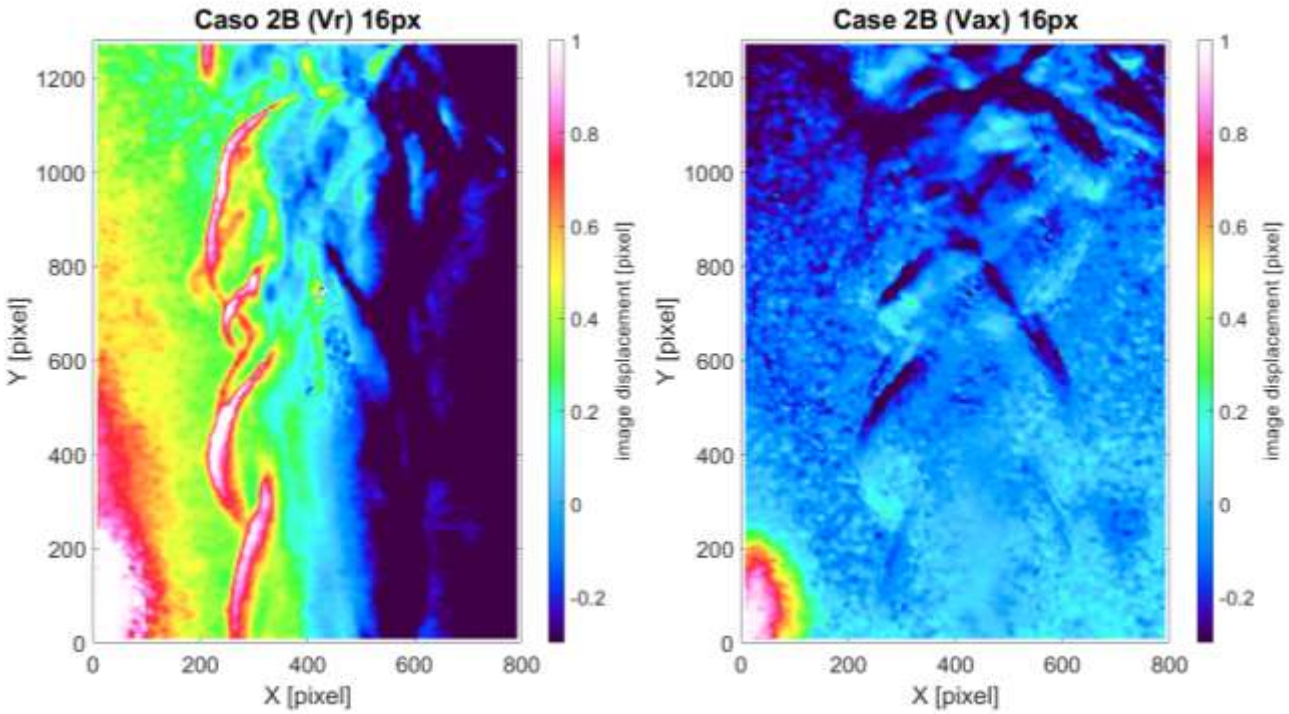

Figure 16 – Radial and axial image displacement for Case 2B (16px)

Case 2C (Figure 17) is the only event in nine where the images do not show a good perspective of the fluid flow.

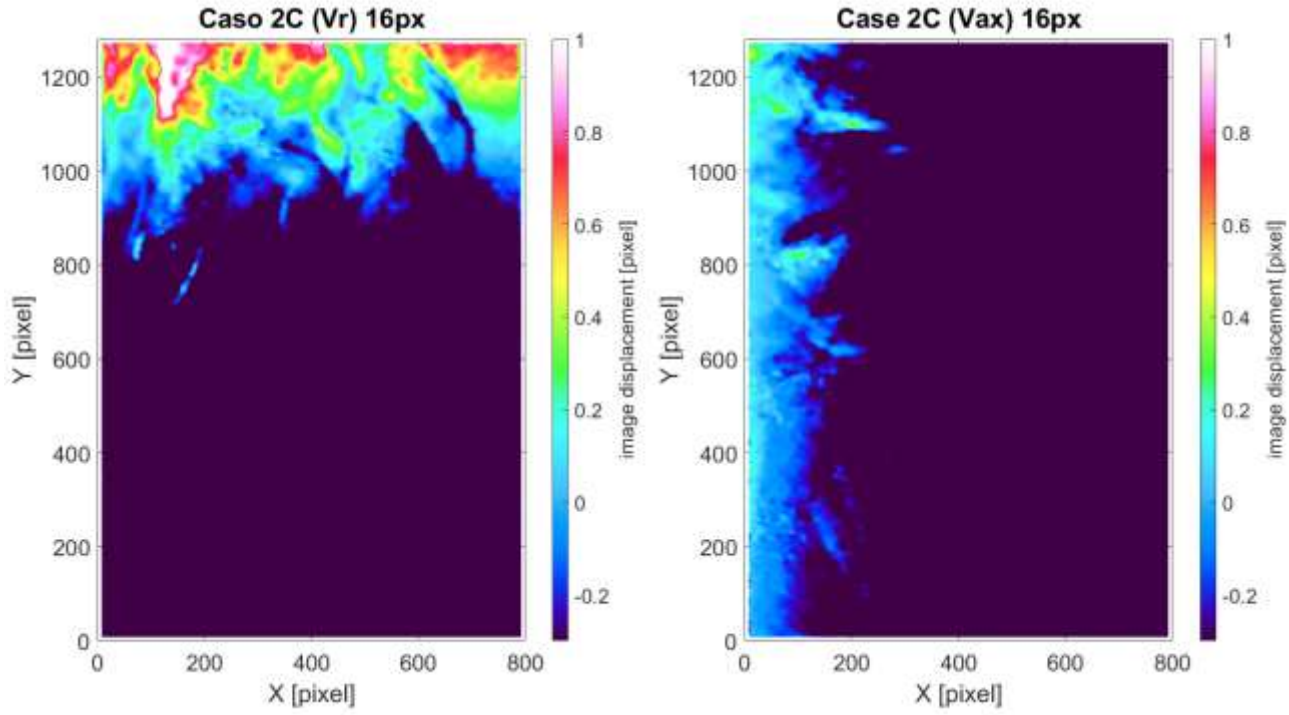

Figure 17 – Radial and axial image displacement for Case 2C (16px)

The last case (Figure 18) shows the bigger turbulence creates by the lifted flame in both radial an axial image displacement.

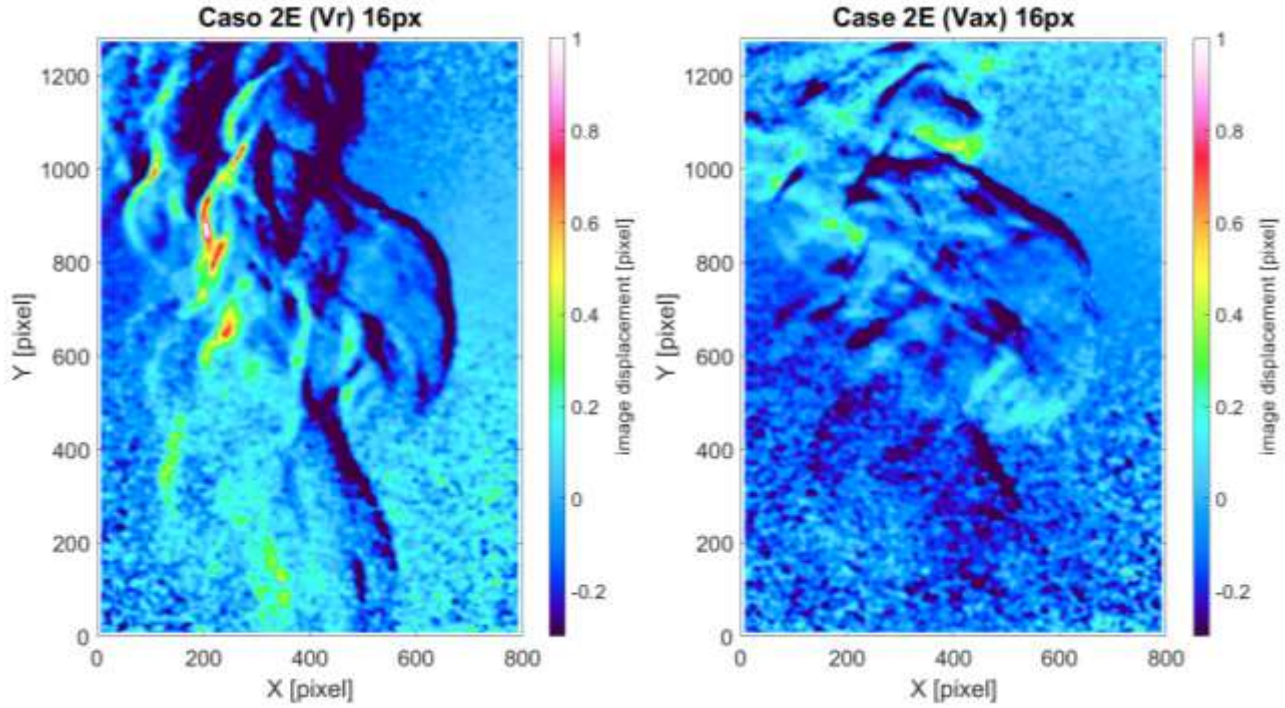

Figure 18 – Radial and axial image displacement for Case 2E (16px)

All four cases are present in Figure 19 and it reveals the discrepancy among cases 2B and 2E, which shows turbulent structures present in radial image displacement that are hard to see in case 2A and not present in case 2C.

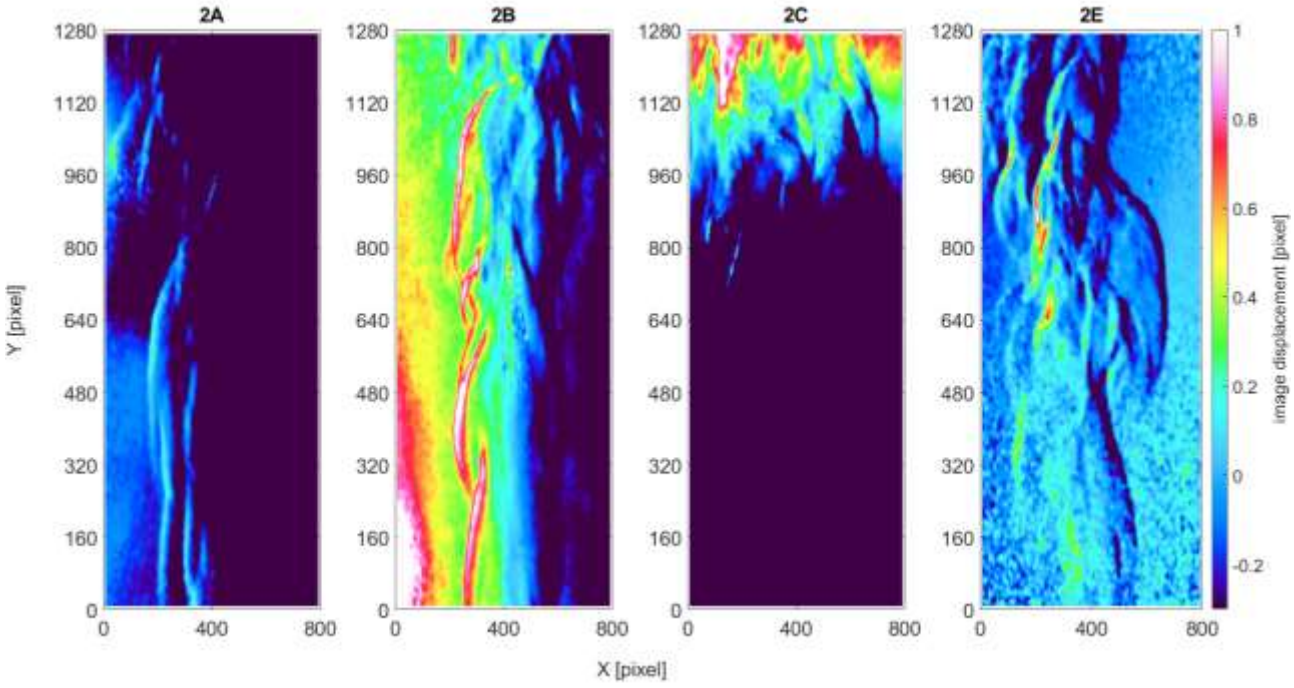

Figure 19 – Multiple cases of lifted flame compared (16px)

Ultimately, the image displacement magnitude for lifted flame events is shown in Figure 20. The image displacement magnitude brought up a new view of the fluid flow, especially for case 2A where the turbulent structures became more

visible. In case 2B there is a small white blur in the region near the X = 400 pixels and Y = 720 pixels because of a pocket shading of flame that appeared in the moment when the picture was recorded.

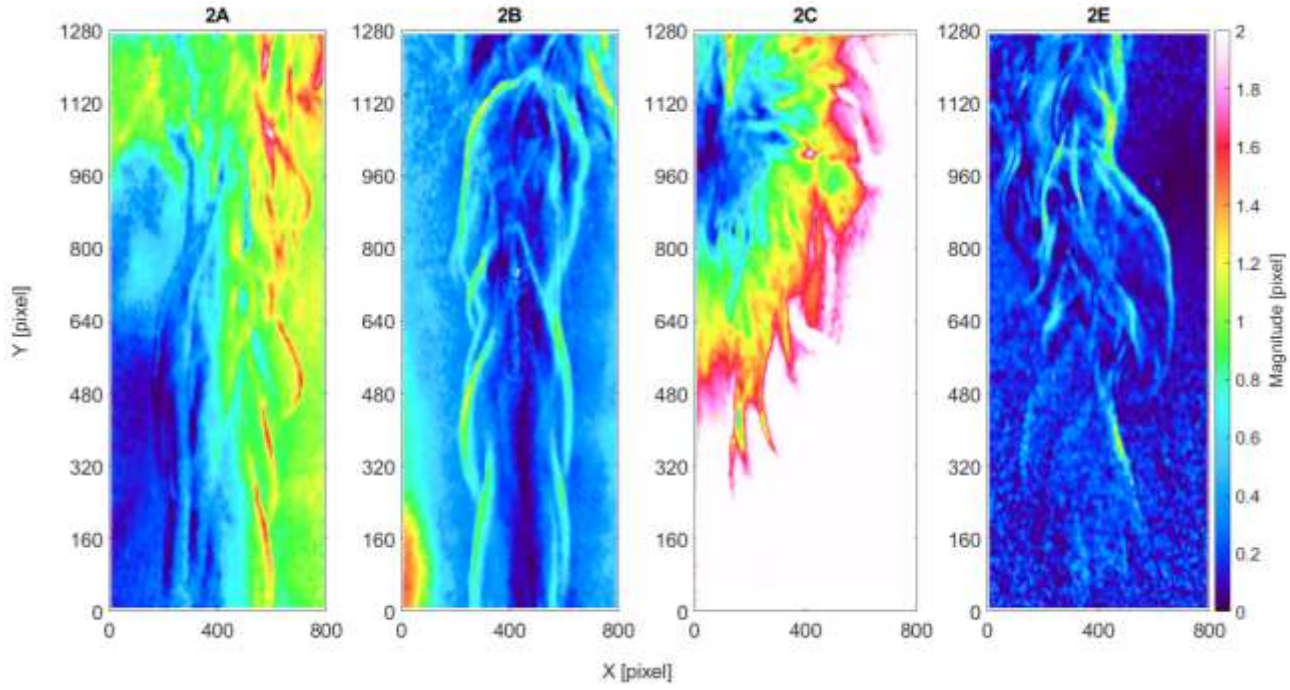

Figure 20 – Image displacement magnitude for multiple lifted flame cases (16px)

Case 2C remained the same, without a good representation of the fluid flow, like the others. Last, the case 2E features the same region that can be encountered in case 1E, the region where the transition between the density changing and the constant density is smooth. Over again, this is caused by the concentrated light reflection of the aluminum sheet where the transparency was attached.

6. CONCLUSIONS

This work analyzed the applicability of the BOS technique in the Yale burner at different flow conditions.

In relation to the background pattern, the white dots in tracing paper (Case B) and the black dots in transparency (Case E) have the best images in all cases. The other cases, A, C and D can be used as well, but if some concerns. For example, in Case 1D the BOS image shows turbulent structures, but in Case 2C it is impossible to see the any density variation, despite of the SNR above 3. In the other hand, there is Case 2A where the radial and axial image displacement images do not show significant turbulent structures, but when the magnitude is ploted the resulting image is similar to the images with the white dots in background.

In the matter of the number of dots, the events with 100 000 dots proved to be better than the 50 000 dots backgrounds, being Case 1D an exception, but this is a special case where the dot size is bigger than the others. The number of dots and its size require more tests to better understand the relation between them and how good the images can be.

Regarding the grid window resolution where PRANA correlates the images, it is easy to notice that the windows of 16 pixels have more information than the 128 pixel windows. This happens because of the number and size of the dots, which fits perfectly in the 16 pixels image.

Similar to PIV, the signal to noise ratio (SNR) is not always the best feedback in BOS because it may induce to errors or to flow visualization that do not represent the real flow. In addition, BOS is also sensitive to problems related to low dynamic velocity range (DRV).

7. ACKNOWLEDGEMENTS

The authors would like to acknowledge Escola Politécnica da Universidade de São Paulo, Fundação de Amparo à Pesquisa do Estado de São Paulo (FAPESP) project number FAPESP 2013/50238-3, FAPESP 2014/50279-4 and Conselho Nacional de Desenvolvimento Cientifico e Tecnológico (CNPq) for the research support.

8. REFERENCES

ADRIAN, R. J.; WESTERWEEL, J. **Particle image velocimetry**. [S.l.]: Cambridge University Press, 2011.
CHIGIER, N. **Combustion Meaasurements**. Philadelphia: Hemisphere Publishing Corporation, 1991. 535 p. ISBN 1-56032-028-1.
DALZIEL, S. B.; HUGHES, G. O.; SUTHERLAND, B. R. Whole-field density measurements by 'synthetic schlieren'. **Experiments in Fluids**, 28, n. 4, 2000. 322-335.
DWORKIN, S. B. et al. Computational and experimental study of a forced, time-dependent, methane–air coflow diffusion flame. **Proceedings of the Combustion Institute**, 31, n. 1, 2007. 971-978.
ECKSTEIN, A. C.; CHARONKO, J.; VLACHOS, P. Phase correlation processing for DPIV measurements. **Experiments in Fluids**, 45, n. 3, 2008. 485-500.
FOND, B. et al. Thermographic Particle Image Velocimetry in flames: current state of the technique. **18th International Symposium on the Application of Laser and Imaging Techniques to Fluid Mechanics**, Lisboa, 4-7 jul. 2016. 13.
GUO(郭广明), G.-M.; LIU(刘洪), H. Density and temperature reconstruction of a flame-induced distorted flow field based on background-oriented schlieren (BOS) technique. **Chinese Physics B**, Shanghai, 26, n. 6, 2017. 064701-1 - 064701-10. DOI: 10.1088/1674-1056/26/6/064701.
HARGATHER, M. J.; SETTLES, G. S. A comparison of three quantitative schlieren techniques. **Optics andLasersinEngineering**, 50, 2012. 8-17.
KOTCHOURKO, N. et al. Concentration measurements in a round hydrogen jet using Background Oriented Schlieren (BOS) technique. **International Journal of Hydrogen Energy**, 39, 2014. 6201-6209.
MAZUMDAR, A. **Systems, Principles and Techniques of Schlieren Imaging**. Columbia University. New York, p. 16. 2013.
MCENALLY, C. S. et al. Computational and experimental study of soot formation in a coflow, laminar ethylene diffusion flame. **Symposium (International) on Combustion**, 1998. 1497-1505.
MOISY, F. **PIVMat toolbox for Matlab**. University Paris-Sud. Paris. 2012. MATLAB program. http://www.fast.u-psud.fr/pivmat.
RAFFEL, M. Background-oriented schlieren (BOS) techniques. **Experiments in Fluids**, 56, 2015. 56-60.
RAFFEL, M.; RICHARD, H.; MEIER, G. E. A. On the applicability of background oriented optical tomography for large scale aerodynamic investigations. **Experiments in Fluids**, 28, n. 5, 2000. 477±481.
SETTLES, G. S.; HARGATHER, M. J. SETTLES, Gary S.; HARGATHER, Michael J. A review of recent developments in schlieren and shadowgraph techniques. **Measurement Science and Technology**, 28, 2017. 042001.

9. RESPONSIBILITY NOTICE

The authors are the only responsible for the printed material included in this paper.